

FIELD-OFF MULTIPLE COULOMB SCATTERING IN THE MICE LIQUID HYDROGEN ABSORBER

G. Chatzitheodoridis*^{1,2}, University of Strathclyde, Department of Physics, Glasgow, UK
¹also at University of Glasgow, Department of Physics and Astronomy, Glasgow, UK
²also at Cockcroft Institute, Warrington, UK
on behalf of The MICE collaboration

Abstract

The Muon Ionization Cooling Experiment (MICE), is a multi-national accelerator physics experiment created to demonstrate Ionization Cooling (IC); a new, rapid beam-cooling technique suitable for the short-lived muon. The performance of IC depends on two key processes - energy loss due to collisional ionization, and Multiple Coulomb Scattering (MCS) - for which accurate models are crucial in enabling quantitative design studies for future muon accelerators. Experimental measurements of MCS of positive muons with momenta in the range 170-240 MeV/c in liquid Hydrogen are reported in this study.

INTRODUCTION

The muon is 207 times more massive than the electron, and is an attractive candidate for future particle physics experiments in part due to reduced bremsstrahlung losses, a factor especially important in a circular beamline setting. High-brightness muon beams are anticipated to be used in High Energy Physics (HEP) for a range of research topics including the precision measurements of the Higgs boson [1,2] and measurement of Charged-Parity (CP) violation in neutrino oscillations [3]. The primary challenge is the particles short life-time (2.2 μ s at rest) and the relatively long cooling periods required by the current techniques to obtain high-brightness beams.

Ionization Cooling

A beam cooling technique that exploits the frictional forces when passing through a low atomic number (Z), high energy absorbent material was first published in [4] and later proposed for application in muon beams [5] as ionization cooling (IC). The technique relies on momentum loss in the transverse and longitudinal directions due to soft ionizing collisions when a focused beam passes through an absorber and is subsequently accelerated through RF-fields. The cooling formula is used to calculate the rate of change of emittance [6]:

$$\frac{d\varepsilon_{\perp n}}{dz} = -\frac{\varepsilon_{\perp n}}{\beta^2 E_{\mu}} \left\langle \frac{dE_{\mu}}{dz} \right\rangle + \frac{\beta_{\perp} (13.6 \text{ MeV}/c)^2}{2m\beta^3 E_{\mu} X_0}, \quad (1)$$

where $\beta = u_{\mu}/c$ with u_{μ} the muon speed, E_{μ} is the energy of the muons, β_{\perp} is one of the Twiss parameters and is minimized at the focus point, m the muon mass and X_0 the

radiation length of the absorber material, which gives rise to the low- Z absorber requirement. The cooling term - first term on the RHS of Eq. (1) - represents emittance reduction due to collisional ionization and the second term on the RHS (heating term) emittance increase due to MCS. At equilibrium emittance where cooling and heating are balanced the net change is zero. MICE recently demonstrated this novel cooling technique in a particle-by-particle measurement of emittance [7]. To evaluate the performance of future proposed facilities, accurate modelling of both collisional ionization and MCS are needed. Although collisional ionization is believed to be well understood, the Muscat collaboration [8] demonstrated that previous versions of GEANT [9] were not compatible with their measurements of MCS. MCS is the phenomenon describing the multiple small-angle scatters a charged particle undergoes when traversing a material. Equation (2) describes the RMS scattering width of the plane projected angle $\theta_{x,y}$ ($y-z$, $x-z$ plane projection respectively) for a beam with momentum p , velocity $\beta = v/c$ traversing z length of material with atomic number Z and X_0 radiation length [10].

$$\theta_{RMS} = \frac{13.6 \text{ MeV}/c}{\beta p} Z \sqrt{\frac{z}{X_0}} \left(1 + 0.038 \frac{zZ^2}{X_0 \beta^2} \right). \quad (2)$$

METHOD

The MICE Apparatus

The muons reaching MICE, are decay products of pions provided by the ISIS proton beam colliding with a titanium target. The captured products are momentum selected by a series of magnets before reaching the MICE channel [11]. The MICE Step IV configuration was used for this analysis comprising of the absorber focus coil (AFC) module - which houses the liquid Hydrogen absorber vessel between two scintillating fibre (Sci-Fi) trackers, upstream (US) and downstream (DS). Three time-of-flight detectors were used to provide velocity measurements (TOF0, 1 & 2). The absorber maintains 21 l of liquid Hydrogen at a temperature of 20 K providing a maximum length of liquid Hydrogen in the beam path of 35 cm [12].

Event Selection

MICE has gathered straight track data with beamline settings configured to provide muon momenta 170, 200 & 240 MeV/c at the absorber, each in two different configurations, with the absorber empty - but in place - and filled

* gavriil.t.chatzitheodoridis@strath.ac.uk

with liquid Hydrogen. The data-sets are initially reduced through a set of selection criteria:

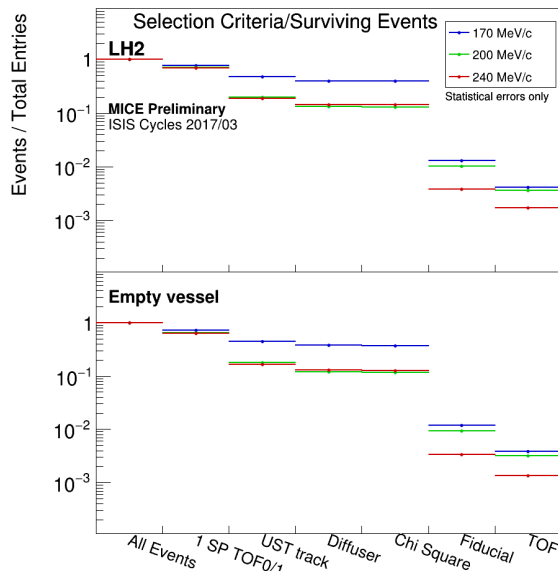


Figure 1: Ratio of events to total number of events (first bin) surviving each cut.

- Only particles that have registered a single TOF0 and TOF1 space-point (SP).
- The particle has a single reconstructed track in the US Sci-Fi tracker.
- The trajectory is estimated to have less than 90 mm radius at the diffuser.
- The track is assessed to be a good fit to the signal clusters formed at the trackers ($\chi^2/NDF < 4$).
- The expected position of the particle at the DS tracker is assessed to be within 100 mm of the beam axis.
- TOF1 and TOF0 provide a transit time that is within a selected range are considered, see Table 1.

The time-of-flight of each particle is assessed between TOF0 and TOF1. The three dominant particle species in the MICE channel are well separated due to momentum conservation, therefore this selection ensures muon beam purity >99%. The quoted momenta for the beams analysed here correspond to the expectation at the absorber from the beamline settings. Explicit calculation of the momenta will be included in future publications. Figure 1 shows the ratio of the total number of events surviving each of the above criteria and Figs. 2, 3 and 4 show the distribution of particles that have passed all other cuts except the one illustrated.

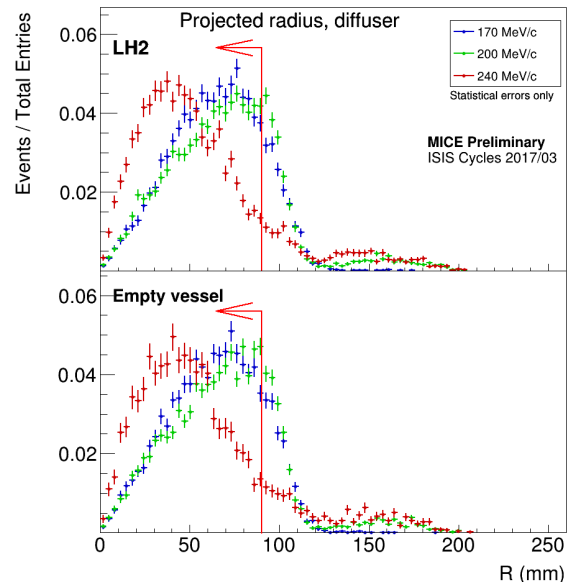


Figure 2: Particles with projected $R = \sqrt{x^2 + y^2} > 90$ mm at the position of the diffuser are rejected.

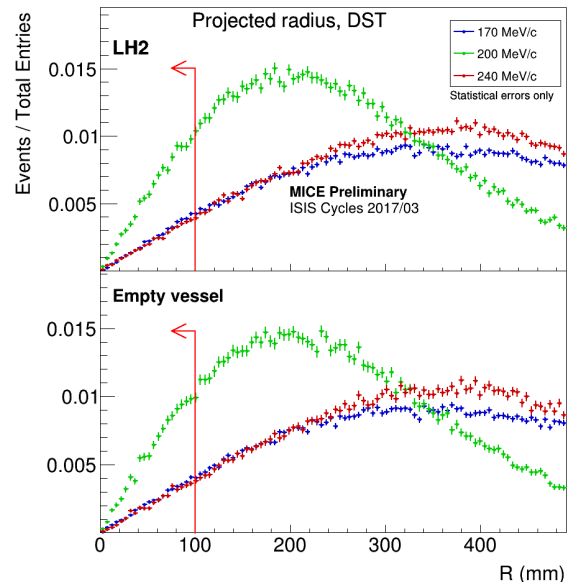


Figure 3: Particles with projected $R = \sqrt{x^2 + y^2} > 100$ mm at the final station of the DS tracker are rejected.

Table 1: Time-of-flight Selection

Beam-setting (MeV/c)	TOF interval (ns)
170	29.07–29.47
240	28.05–28.45
240	27.33–27.73

RESULTS

The resulting scattering distributions (Figs. 5 and 6) are expressed as the difference of angles between the US and

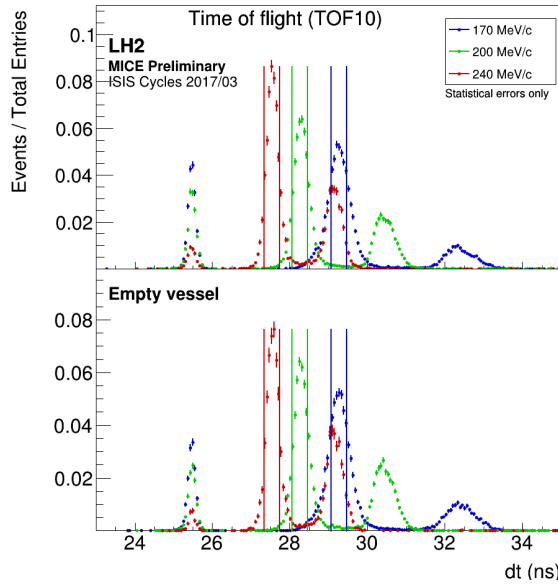


Figure 4: Time-of-flight distribution with selection intervals.

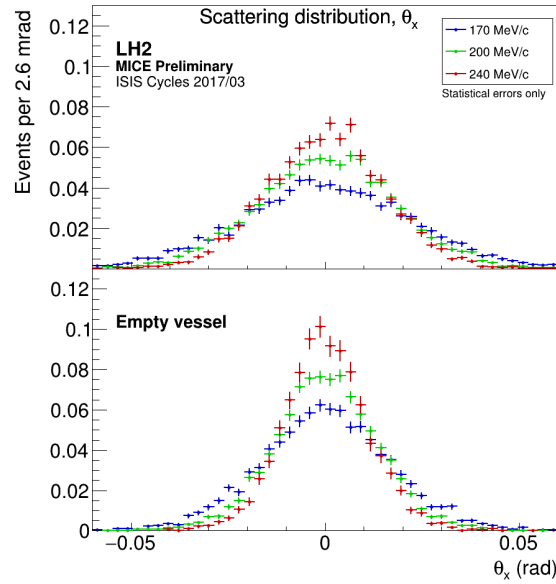


Figure 5: Distribution of θ_x for the three momenta settings. For vessel full (top) and empty (bottom) configurations.

DS momentum vectors (\vec{P}_{US} , \vec{P}_{DS}) when projected into corresponding orthogonal planes. The first plane is defined as the plane containing the US vector and the Y experimental axis, and the second plane is defined as its orthogonal. This means that the two planes required for the projected angle calculations are defined on a particle by particle basis. This definition would be equal to using the Y-Z and X-Z planes (from experimental coordinates) if all particles moved parallel to the experimental Z-axis. Because this is not the case the following definitions are established for scattering studies:

$$\theta_y = \arctan\left(\frac{\vec{P}_{DS} \cdot (\hat{Y} \times \vec{P}_{US})}{|\hat{Y} \times \vec{P}_{US}| |\vec{P}_{DS}|}\right) \quad (3)$$

$$\theta_x = \arctan\left(\frac{\vec{P}_{DS} \cdot (\vec{P}_{US} \times (\hat{Y} \times \vec{P}_{US}))}{|\vec{P}_{US} \times (\hat{Y} \times \vec{P}_{US})| |\vec{P}_{DS}|}\right). \quad (4)$$

CONCLUSIONS & FUTURE WORK

This paper presents experimental measurements of MCS of muons crossing a mean of 33 cm of liquid Hydrogen (Figs. 5 and 6 top), with beam momenta 170, 200 and 240 MeV/c in the MICE channel. The same measurement with identical selection criteria is performed with the liquid Hydrogen vessel empty. The scattering distributions for the empty absorber configuration (Figs. 5 and 6 bottom) shows the scattering of particles from the intermediate material of the trackers and vessel, mainly Aluminium, scintillator material (BCF-10 plastic fibres) and Helium. The top row shows the added effect of liquid Hydrogen. The decrease in width can be observed as the beam momenta increases, whilst the width increases at all settings when liquid Hydrogen is added in the beam path. The future aim of this analysis is to compare the observations with the predictions of GEANT and the Moliere [13] MCS model.

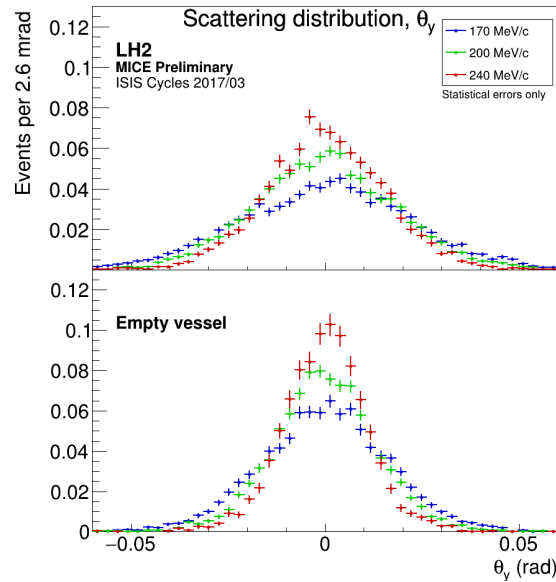


Figure 6: Distribution of θ_y for the three momenta settings. For vessel full (top) and empty (bottom) configurations.

REFERENCES

- [1] D. V. Neuffer, Y. I. Alexahin, M. A. Palmer, C. M. Ankenbrandt, and J.-P. Delahaye, "A Muon Collider as a Higgs Factory", in *Proc. 4th Int. Particle Accelerator Conf. (IPAC'13)*, Shanghai, China, May 2013, paper TUPFI056, pp. 1472–1474.
- [2] M. Chiesa, F. Maltoni, L. Mantani, B. Mele, F. Piccinini, and X. Zhao, "Measuring the quartic higgs self-coupling at a multi-TeV muon collider", 2020. [arXiv:2003.13628](https://arxiv.org/abs/2003.13628)
- [3] A. D. Rujula, M. Gavela, and P. Hernández, "Neutrino oscillation physics with a neutrino factory", *Nucl. Phys. B*,

- vol. 547, pp. 21–38, 1999. doi:10.1016/S0550-3213(99)00070-X
- [4] Y. M. Ado and V. I. Balbekov, “Use of ionization friction in the storage of heavy particles”, *Sov. Atom. Energ.*, vol. 31, pp. 731–736, 1971. doi:10.1007/BF01123390
- [5] D. Neuffer, “Principles and Applications of Muon Cooling”, *Part. Accel.*, vol. 14, pp. 75–90, 1983. doi:10.1063/1.49353
- [6] D. Neuffer, “Introduction to muon cooling”, *Nucl. Instrum. Meth. Sec. A*, vol. 532, pp. 26–31, 2004. doi:10.1016/j.nima.2004.06.051
- [7] MICE Collaboration, “Demonstration of cooling by the Muon Ionization Cooling Experiment”, *Nature*, vol. 578, pp. 53–59, 2020. doi:10.1038/s41586-020-1958-9
- [8] Muscat Collaboration, “The scattering of muons in low Z materials”, *Nucl. Instrum. Meth. Sec. A*, vol. 83, pp. 492–504, 2005. doi:10.1016/j.nimb.2006.05.006
- [9] S. Agostinelli *et al.*, “Geant4—a simulation toolkit”, *Nucl. Instrum. Methods Phys. Res. A*, vol. 506, no. 3, pp. 250–303, 2003. doi:10.1016/S0168-9002(03)01368-8
- [10] M. Tanabashi *et al.*, “Review of particle physics”, *Phys. Rev. D*, vol. 98, p. 030001, 2018. doi:10.1103/PhysRevD.98.030001
- [11] M. Bogomilov *et al.*, “The MICE Muon Beam on ISIS and the beam-line instrumentation of the Muon Ionization Cooling Experiment”, *J. Inst.*, vol. 7, pp. 5009–5009, 2012. doi:10.1088/1748-0221/7/05/p05009
- [12] V. Bayliss *et al.*, “The liquid-hydrogen absorber for MICE”, *J. Inst.*, vol. 13, pp. 9008–9008, 2018. doi:10.1088/1748-0221/13/09/t09008
- [13] H. A. Bethe, “Molière’s theory of multiple scattering”, *Phys. Rev. E*, vol. 89, pp. 1256–1266, 1953. doi:10.1103/PhysRev.89.1256